Research and development attempt of a new type of glass bead retroreflective material that can reduce the downward reflection for UHI mitigation

P. Rajagopalan, V. Soebarto and H. Akbari (Eds.), *6th International Conference on Countermeasures to Urban Heat Islands (IC2UHI)*, pp. 80-88. ©2023, RMIT University, Melbourne, Australia.

Research and development attempt of a new type of glass bead retro-reflective material that can reduce the downward reflection for UHI mitigation

Jihui Yuan[1,2], *Yasuhiro Shimazaki*[2], *Shingo Masuko*[3], *Masaki Tajima*[2], *Jiale Chai*[4], *Craig Farnham*[1], *Kazuo Emura*[1], *Marko Bizjak*[5]
[1]*Osaka Metropolitan University, Osaka, Japan*
[2]*Toyohashi University of Technology, Toyohashi, Japan*
[3]*NOMURA Co. Ltd,, Tokyo, Japan*
[4]*The Hong Kong Polytechnic University, Hong Kong, China*
[5]*University of Maribor, Maribor, Slovenia*

ABSTRACT

This paper explores the use of retro-reflective (RR) materials on exterior walls to reduce urban heat island (UHI) effects. However, some research indicates that these materials can increase reflected downward solar radiation, worsening the UHI when the solar altitude is high. To address this, the paper introduces a new glass bead RR material (NDGB) designed to reduce downward reflection. The paper evaluates the NDGB-RR material through lab optical reflectance and outdoor small-scale wall-model measurements, comparing its angular retro-reflectance and angular reflection-intensity distribution to normal glass bead (NGB) RR and capsule RR materials. Results show that the NDGB-RR material has similar angular retro-reflectance to the NGB-RR and capsule RR materials but significantly reduces downward reflection at angles over 60 degrees, by approximately 97% and 98%, respectively. Overall, this research presents a promising solution to mitigate the negative impact of RR materials on UHI through the use of the NDGB-RR material. By reducing reflected downward solar radiation, this material can potentially alleviate UHI effects when used on building exterior walls.

Keywords: Glass bead retro-reflective material, Upward-downward reflection, Lab optical experiment, Outdoor small-scale wall-model.

Introduction

The urban heat island (UHI) phenomenon has significantly intensified over time, resulting in heightened risks of heat-related mortality and increased energy consumption for air-conditioning purposes (Manoli et al., 2019; Li and Zhao, 2012; Solecki et al., 2005). Moreover, the UHI exerts a detrimental influence on the outdoor thermal comfort experienced

[1] Corresponding Author: [yuan@omu.ac.jp], ORCID: 0000-0002-1608-9973
[2] [shimazaki@ace.tut.ac.jp], ORCID: 0000-0002-7517-756X
[3] [s.masuko@nomura.jp], ORCID:
[4] [masaki.tajima.qt@tut.jp], ORCID:
[5] [jiale.chai@polyu.edu.hk], ORCID: 0000-0001-6450-3190
[6] [farnham@omu.ac.jp], ORCID: 0000-0002-8822-891X
[7] [emuraocu@gmail.com], ORCID:
[8] [m.bizjak@um.si], ORCID:

by individuals (Livada et al., 2002). Various studies have demonstrated that the intensity of UHI has experienced a surge in regions characterized by a humid climate, such as Eastern China (Liao et al., 2018), the central part of Nagoya, Japan (Kato and Yamaguchi, 2005), urban areas in the United States (Imhof et al., 2010), and the European Union (Zhou et al., 2013).

Numerous strategies have been implemented globally to tackle the escalating the UHI phenomenon. One notable approach involves the development and utilization of highly reflective (HR) building coating materials. However, it is important to note that the majority of HR materials currently in use are classified as diffuse HR (DHR) materials, resulting in the absorption of incident solar radiation by urban surfaces (Rossi et al., 2015; Yuan et al., 2014). Consequently, alternative solutions and advancements are necessary to address this limitation and optimize the effectiveness of HR materials in mitigating UHI effects.

Extensive advancements have been made in the development of retro-reflective (RR) materials, which offer a promising solution for mitigating the UHI phenomenon by effectively reflecting incident solar radiation towards the sky, preventing absorption. The advantages of RR materials have been thoroughly investigated through comprehensive simulation research and optical experiments. Among these investigations, a glass bead with a refractive index of 1.9 has emerged as the most efficient medium for retro-reflecting incident light in the desired direction (Yuan et al., 2015). To evaluate the impact of RR materials on the outdoor radiation-environment indicators, such as wet bulb globe temperature (WBGT), sol-air temperature (SAT), and change operative temperature (COT), field measurements have been carried out (Yuan et al., 2022).

Nevertheless, it is crucial to acknowledge that the performance of RR materials is subject to limitations. Specifically, when the incident angle of light surpasses approximately 50 degrees, the efficacy of RR materials diminishes, and there is a noticeable escalation in the downward reflection component, particularly when RR materials are applied to building facades (Rossi et al., 2014; Levinson et al., 2020). This phenomenon adversely affects pedestrians and exacerbates the UHI effect. Consequently, in order to alleviate the negative impact of downward reflection caused by RR materials, as depicted in Figure 1, the implementation of an appropriate technical method becomes imperative.

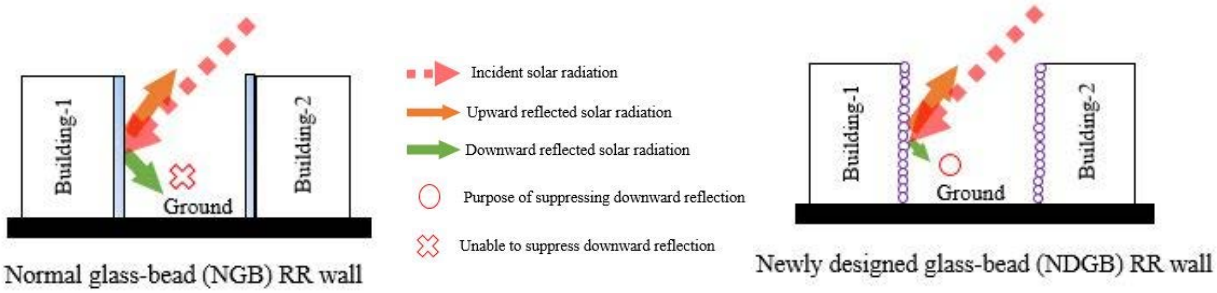

Figure 1. The newly designed glass-bead (NDGB) RR material is an innovation that effectively mitigates downward solar reflection; left side is the normal glass-bead (NGB) RR sample, while the right side is the NDGB-RR sample.

Materials and Methodology

In this study, an optical experiment was conducted in a laboratory to assess the angular retro-reflectance and angular reflection intensity distribution of three RR samples, including a normal glass-bead (NGB) RR sample; a newly designed glass-bead (NDGB) RR sample, where a silver reflective material coated one-eighth of the surface of the NGB RR

sample; and a capsule RR sample. Additionally, an outdoor small-size wall-model experiment was carried out to determine and compare the upward and downward reflection ratios of the three RR samples.

NDGB-RR sample

To create the NDGB-RR samples, this study adopted transparent glass beads with a refractive index of 1.9 and a particle size of 1.0 cm, as previously suggested in Yuan et al. (2016a). As per previous research by Yuan et al. (2021), the position of the downward specular reflection from inside the glass beads was calculated, and one-eighth of the glass bead's coating area was determined. To achieve a specular reflection function inside the glass bead, the study employed a silver pen paint, as recommended in Yuan et al. (2016b), which had a measured solar reflectance around 0.7 and was used to coat one-eighth of the glass bead's bottom area. The surface photo of the three types of RR samples used in this study, namely NGB, NDGB, and capsule, are presented in Figure 2.

(**i**) NGB-RR sample (**ii**) NDGB-RR sample (**iii**) Capsule-RR sample

Figure 2. The surface photo of the three RR samples, (**i**) NGB-RR sample; (**ii**) NDGB-RR sample, and (**iii**) Capsule-RR sample.

Lab optical experiment

This study utilized an emitting-receiving optical fiber apparatus, as shown in Figure 3, which included a halogen lamp (wavelength range: 360-1700 nm, and bulb color temperature: 2800 K), spectrophotometers for both visible (wavelength range: 400-1100 nm) and infrared (wavelength range: 900-1715 nm) bands, an emitting optical fiber probe and a receiving optical fiber probe with wavelength range of 400-2100 nm, and probe ferrule diameter of 6.36 mm, and a sample stage for adjusting the sample surface height.

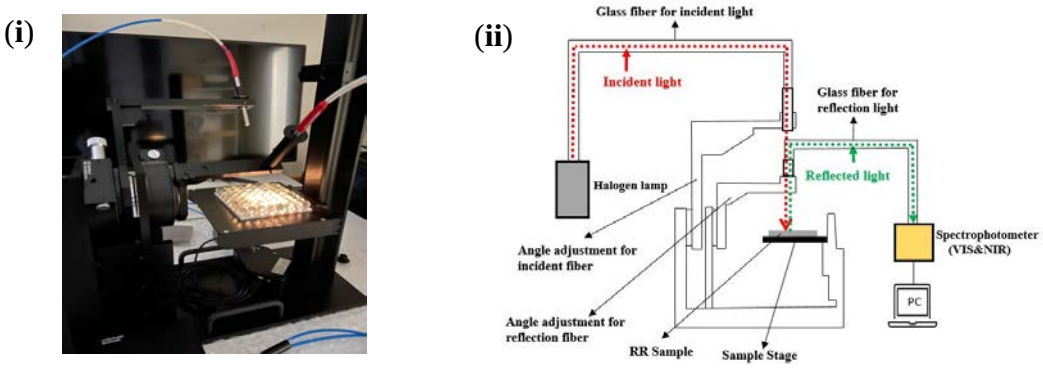

Figure 3. The emitting–receiving optical fiber apparatus, (i) is for photographs of the optical apparatus; and (ii) is for the conceptual drawings of the optical apparatus.

The angular retro-reflectance and angular reflection intensity distribution of the three RR samples were measured at different incident angles. In the optical experiment, the distance from the optical fiber probe to the RR sample surface was set at 30 mm. The two axes of the emitting-receiving optical fiber apparatus, one for light-emitting and the other for light-receiving, could be manually adjusted to any desired angle for ease of measurement. Additionally, the apparatus was designed to minimize the effects of incident and reflected light mixing.

Outdoor small-size wall-model experiment

The small-size wall-model used to determine the upward and downward reflection ratios of the three different RR building walls that were exposed to the actual solar radiation environment is shown in Figure 4.

The dimensions of the wall-model were H=150 mm, D=150 mm, and W=100 mm. Solar radiation measurements were taken using pyranometers with a wavelength range of 300–2000 nm and a measured solar-irradiance range of 0–2000 W/m^2, with a deviation of ± 50 W/m^2. The accuracy of the guaranteed temperature range was −30–70 °C. The outdoor small-size wall-model experiment was conducted in Toyohashi, Japan, on sunny day of summer, 24 June 2021, from JST 10 am to 4 pm. The urban aspect ratio (H/D), which is the building model height (H) compared to the distance between two building models (D), was set to 1.0 for this experiment.

In order to determine the upward and downward reflection ratios of the three RR wall-models, we also created a same size model with completely black vertical walls. This black wall-model was used to modify the reflection ratios of the three RR wall-models. Additionally, all of the wall-models were placed on top of a deep gray sheet plate with a relatively low solar reflectance of approximately 0.05 for the exposure experiment.

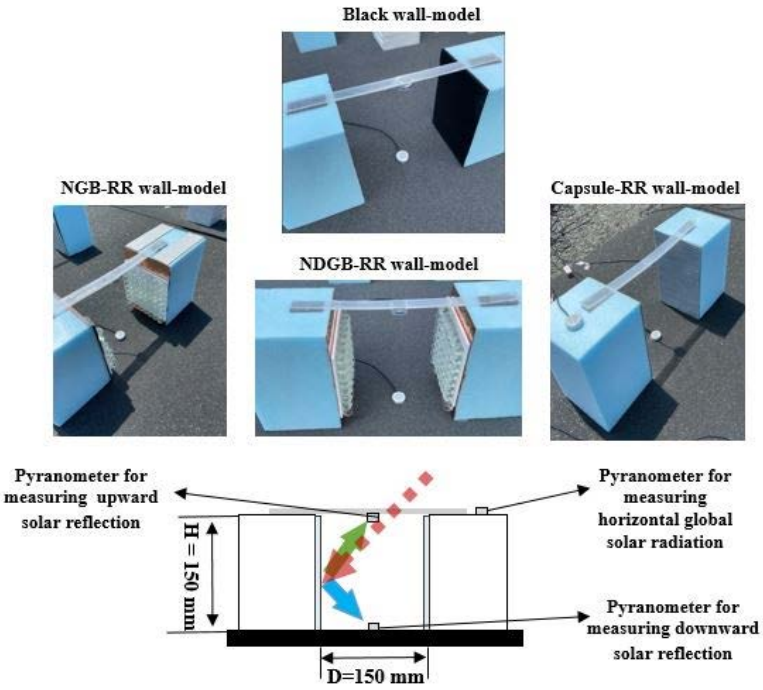

Figure 4. The small-size wall-model with H=150 mm, D=150 mm and W=100 mm, exposed to the actual radiation-environment for measuring the upward and downward reflection ratios of three RR wall-models.

The upward and downward reflection ratios of the RR wall-models were determined using Equation (1)–(4).

$$E_{w\downarrow} = E_{m\downarrow}(wall) - E_{m\downarrow}(Black\ wall) \quad (1)$$

$$E_{w\uparrow} = E_{m\uparrow}(wall) - E_{m\uparrow}(Black\ wall) \quad (2)$$

$$R_{w\downarrow} = 100 \times E_{w\downarrow} / E_h \quad (3)$$

$$R_{w\uparrow} = 100 \times E_{w\uparrow} / E_h \quad (4)$$

where $E_{w\downarrow}$ is the modified downward reflection of the RR wall-models [W/m^2], $E_{w\uparrow}$ is the modified upward reflection of the RR wall-models [W/m^2], E_h is the measured horizontal solar radiation [W/m^2], $E_{m\downarrow}(wall)$ is the downward reflection of the RR wall-models [W/m^2], $E_{m\downarrow}(Black\ wall)$ is the downward reflection of the black wall-model [W/m^2], $E_{m\uparrow}(wall)$ is the upward reflection of the RR wall-models [W/m^2], $E_{m\uparrow}(Black\ wall)$ is the upward reflection of the black wall-model [W/m^2], $R_{wa\downarrow}$ is the downward reflection ratio of the RR wall-models [%], and $R_{w\uparrow}$ is the upward reflection ratio of the RR wall-models [%].

Results and Discussion

Comparison of angular retro-reflectance

The emitting-receiving optical fiber apparatus was used to assess the angular retro-reflectance of three different RR samples: NGB, NDGB, and Capsule. Figure 5 displays the results obtained from this evaluation.

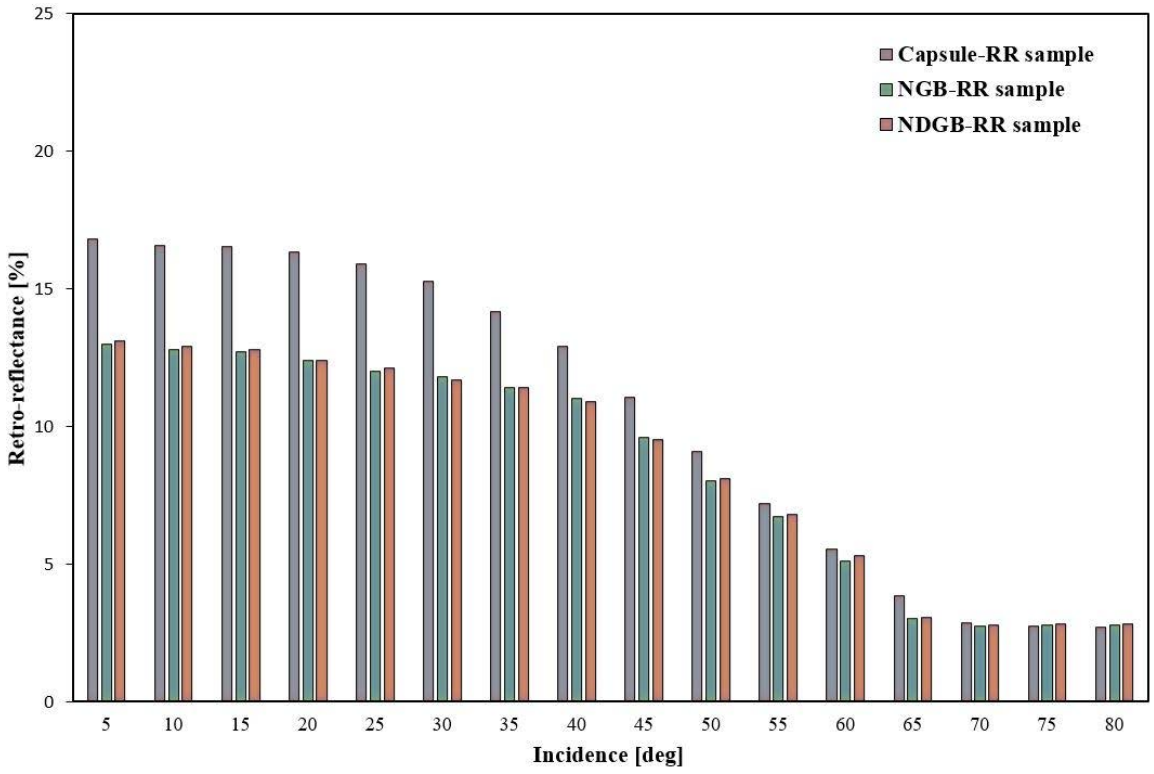

Figure 5. Angular retro-reflectance of RR samples (NGB, NDGB, Capsule), evaluated using the emitting–receiving optical fiber apparatus.

The Capsule-RR sample, which is currently available on the market, demonstrated an average angular retro-reflectance approximately 1.9% higher than the other two glass-bead RR samples, NGB and NDGB. The angular retro-reflectance of the NGB and NDGB samples was nearly identical, with a small difference of only approximately 0.04%. Additionally, the results indicated that the angular retro-reflectance of all three RR samples was heavily influenced by the incident angles of light. Specifically, as the incident angle of light increased, the angular retro-reflectance tended to decrease, particularly when the incident angle surpassed 60 degrees. At this point, the angular retro-reflectance became quite weak.

Comparison of angular reflection intensity

Figure 6 depicts the angular reflection intensity measurements at various incident angles (10 degrees, 30 degrees, 60 degrees, and 80 degrees) for the NGB-RR, NDGB-RR, and capsule-RR samples.

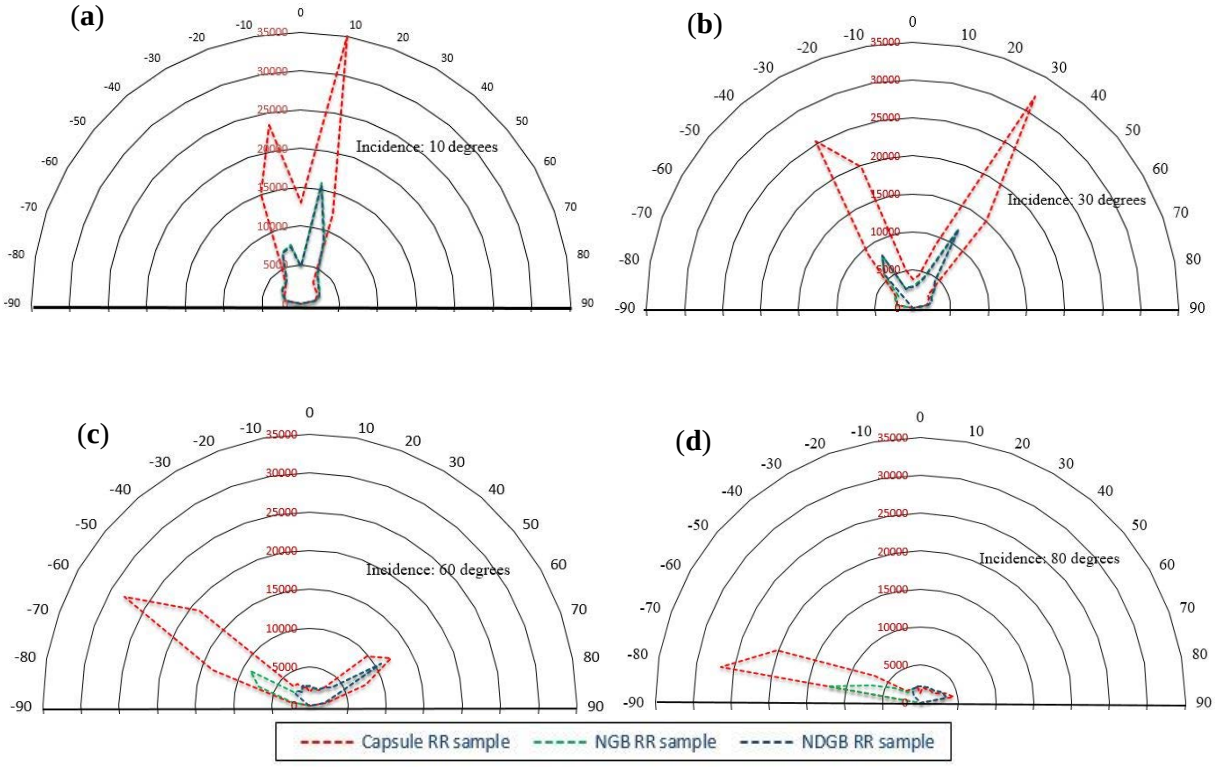

Figure 6. Measured angular reflection intensity distribution of NGB-RR, NDGB-RR, and Capsule-RR samples at various incident angles; (**a**) is for incidence of 10 degrees, (**b**) is for incidence of 30 degrees, (**c**) is for incidence of 60 degrees, and (**d**) is for incidence of 80 degrees.

The capsule-RR sample exhibited greater retro-reflection intensity than the other two developed glass-bead RR samples at light incident angles of 10 degrees and 30 degrees, while their retro-reflection intensities were nearly equal when the incident angle increased to 60 degrees and 80 degrees. Furthermore, irrespective of the light incident angles, the capsule-RR sample displayed stronger negative reflection (downward specular reflection) intensity than the other two glass-bead RR samples. Additionally, when the incident angle surpassed 30 degrees, the negative reflection intensity of the NDGB-RR sample became notably weaker compared to that of the NGB-RR and capsule-RR samples.

Comparison of upward and downward reflection ratios

On June 24th, 2021 in Toyohashi City, Japan, Figure 7 displays the results of upward and downward reflection ratios of three RR small-size wall-models during a sunny day.

The upward reflection ratios of the three RR wall-models were almost identical, exhibiting only a 0.62% difference. However, the downward reflection ratios showed a difference among the three RR wall-models. The NGB-RR wall-model exhibited only a 0.3% smaller ratio than the capsule-RR wall-model, while the NDGB-RR wall-model had a downward reflection ratio of about 5.4% and 5.0% less than the capsule-RR and NGB-RR walls, respectively, on June 24th. The largest differences in hourly downward reflection ratios among the three RR wall-models were recorded at JST 4 pm on June 24th, with approximately 9.5% (NGB & Capsule > NDGB) differences.

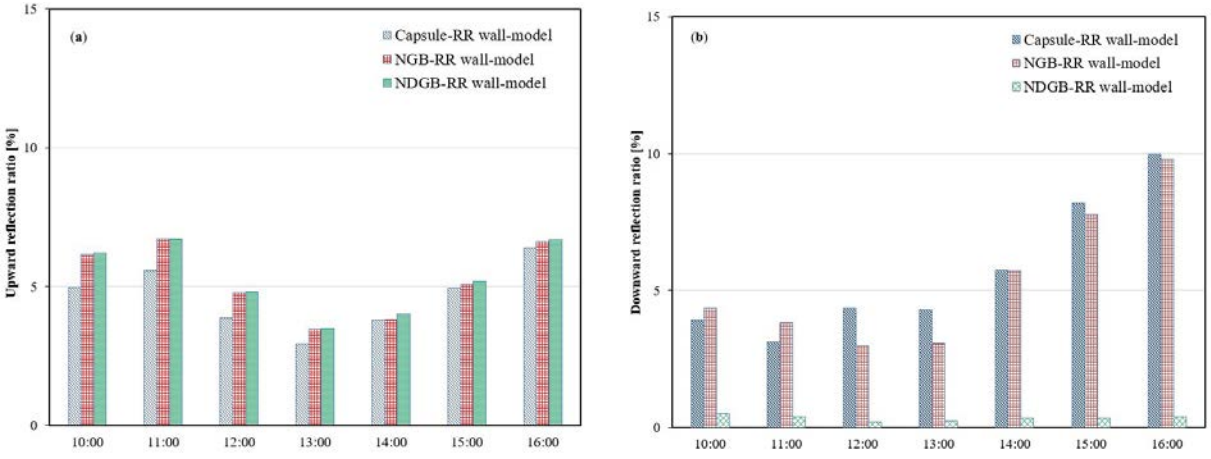

Figure 7. Evaluated hourly upward and downward reflection ratios of three RR wall-models; (a) is for upward reflection ratios, and (b) is for downward reflection ratios of the three RR wall-models on 24 June, 2021, from JST 10 am to 4 pm.

Discussion

The results of measuring the angular retro-reflectance of three RR samples using an emitting-receiving optical fiber apparatus revealed that the capsule-RR sample had the highest angular retro-reflectance, being on average 2.5% higher than that of the NGB and NDGB RR samples at incident angles below 60 degrees. However, when the incidence exceeded 60 degrees, the angular retro-reflectance of all three RR samples became very small and almost identical. These results are consistent with previous studies (Rossi et al. 2014; Yoshida and Mochida 2018), which have shown that retro-reflectance gradually decreases, especially above a 60 degrees elevation angle. The NDGB-RR sample had almost the same angular retro-reflectance as the NGB-RR sample, even though only one-eighth of the surface of the NGB RR sample was coated with a silver reflective material.

Analysis of the angular reflection intensity distribution of the three RR samples revealed that the capsule-RR sample exhibited stronger retro-reflection and specular negative reflection behaviors than the NGB-RR and NDGB-RR samples at low incidence of 10 and 30 degrees. At higher incident angles of 60 and 80 degrees, the specular negative reflection of the capsule-RR sample increased significantly compared to the low incidences, and its RR behavior was almost lost at the incidence of 80 degrees. The RR behavior of the NGB-RR and NDGB-RR samples was almost identical at all incidences of light, and the specular negative reflection of the NDGB-RR sample weakened significantly when the incidence of light exceeded 60 degrees. These findings suggest that the NDGB-RR material developed in this

study could reduce the specular negative reflection and enhance its potential for reducing the downward specular negative reflection of building walls when applied to building facades.

The results of the RR wall-model experiment indicated that the upward reflection ratios of the three RR wall-models were almost the same during the sunny day, which is consistent with previous simulation measurements (Yuan et al. 2021). However, the capsule-RR material (currently available on the market) showed significantly stronger specular downward reflection than the NGB-RR materials, which can negatively impact the outdoor environment, particularly on sunny days with a lower sun elevation. When comparing the NGB-RR and NDGB-RR wall-models, the NDGB-RR material significantly reduced the specular downward reflection component by approximately 97%, without affecting the original retro-reflectance, when a suitable technique of coating the surface of NGB-RR material was used. Thus, the NDGB-RR sample developed in this study has the potential to reduce the downward reflection from building facades and mitigate the UHI phenomenon.

Limitations

The limitations of this study can be summarized as follows. Firstly, the optical apparatus used in this study, which consisted of an emitting-receiving optical fiber system, was limited to measuring the two-dimensional reflection of the RR samples due to the presence of only one ray axis for measuring reflections. Secondly, the measurements of upward and downward reflection ratios for the small-size building-wall models exposed to the external environment were susceptible to variations in solar radiation stability and influenced by the surrounding environment. Thirdly, due to the need to allow incident sunlight into the building-wall model space, only one pyranometer was placed respectively on the upper and lower-middle portions of the building-wall model, which may have been insufficient to accurately measure the upward and downward reflection ratios of the building walls.

Conclusions and future work

This study created an NDGB-RR sample by applying silver reflective materials to one-eighth of the surface of an NGB-RR sample. The directional reflection characteristics were evaluated using optical measurements and an outdoor small-size wall-model experiment. The capsule-RR sample had the largest angular retro-reflectance, and stronger RR and specular negative reflection behaviors compared to the NGB-RR and NDGB-RR samples. The NGB-RR and NDGB-RR samples had similar RR behaviors regardless of the incident angle, but the NDGB-RR sample reduced the specular downward reflection component of the building wall to a great extent without affecting the retro-reflectance. The upward reflection ratios of the three RR wall-models were almost the same during the experimental sunny day.

Our planned future work will focus on two main objectives. Firstly, we will develop an emitting-receiving optical fiber apparatus capable of measuring the directional reflection characteristics of three-dimensional reflections. Secondly, we aim to improve the wall-model by reducing the influence of external uncertainties to accurately evaluate the upward and downward reflection ratios of different reflection directional building walls.

Acknowledgments

The authors are sincerely grateful to the “JSPS KAKENHI (Grant Number: JP22K02098)” and “The Naito Research Grant” for their support.

References

Imhof, ML., Zhang, P., Wolfe, R. E. & Bounoua, L. (2010). Remote sensing of the urban heat island effect across biomes in the continental USA. *Remote Sens. Environ.*, 114, 504–513.

Kato, S., Yamaguchi, Y. (2005). Analysis of urban heat-island effect using ASTER and ETM+ Data: Separation of anthropogenic heat discharge and natural heat radiation from sensible heat flux. *Remote Sensing of Environment*, 99(1-2), 44–54.

Levinson, R., Chen, S., Slack, J., Goudey, H., Harima, T., Berdahl, P. (2020). Design, characterization, and fabrication of solar-retroreflective cool-wall materials. *Solar Energy Materials and Solar Cells*, Vol.206, 110117.

Li, Y., Zhao, X. (2012). An empirical study of the impact of human activity on long-term temperature change in China: A perspective from energy consumption. *Journal of Geophysical Research*, 117 (D17): D17117.

Liao, W. et al. (2018). Stronger contributions of urbanization to heat wave trends in wet climates. *Geophys. Res. Lett.*, 45, 11310–11317.

Livada, I., Santamouris, M., Niachou, K., Papanikolaou, N., Mihalakakou, G. (2002). Determination of places in the great Athens area where the heat island effect is observed. *J. Theor. Appl. Climatol.*, 71, 219–230.

Manoli, G., Fatichi, S., Schläpfer, M. et al. (2019). Magnitude of urban heat islands largely explained by climate and population. *Nature*, 573, 55–60.

Rossi, F., Castellani, B., Presciutti, A., Morini, E., Filipponi, M., Nicolini, A., Santamouris, M. (2015). Retroreflective facades for urban heat island mitigation: Experimental investigation and energy evaluations. *Applied Energy*, 145, 8-20.

Rossi, F., Pisello, AL., Nicolini, A., Filipponi, M., Palombo, M. (2014). Analysis of retro-reflective surfaces for urban heat island mitigation: A new analytical model. *Applied energy*, 114, 621-631.

Solecki, W.D., Rosenzweig, C., Parshall, L., Pope, G., Clark, M., Cox, J., Wiencke, M. (2005). Mitigation of the heat island effect in urban New Jersey. *Global Environmental Change Part B: Environmental Hazards*, 6 (1), 39–49.

Yoshida, S., Mochida, A. (2018). Evaluation of effects of windows installed with near-infrared rays retro-reflective film on thermal environment in outdoor spaces using CFD analysis coupled with radiant computation. *Building Simulation*, 11(5), 1053-1066.

Yuan, J., Emura, K., Farnham, C. A method to measure retro-reflectance and durability of retro-reflective materials for building outer walls. *Journal of Building Physics*, 2014, 38(6), 500-516.

Yuan, J., Emura, K., Farnham, C., Sakai, H. (2016a). Application of glass beads as retro-reflective facades for urban heat island mitigation: experimental investigation and simulation analysis. *Building and Environment*, 105, 140-152.

Yuan, J., Emura, K., Sakai, H., Farnham, C., Lu, S. (2016b). Optical analysis of glass bead retro-reflective materials for urban heat island mitigation. *Solar Energy*, 132, 203-213.

Yuan, J., Farnham, C., Emura, K. (2015). Geometrical-optics analysis of reflective glass beads applied to building coatings. *Solar Energy*, 122, 997-1010.

Yuan, J., Farnham, C., Emura, K. (2021). Evaluation of retro-reflective properties and upward to downward reflection ratio of glass bead retro-reflective material using a numerical model. *Urban Climate*, 36, 100774.

Yuan, J., Masuko, S., Shimazaki, Y., Yamanaka, T., Kobayashi, T. (2022). Evaluation of outdoor thermal comfort under different building external-wall-surface with different reflective directional properties using CFD analysis and model experiment. *Building and Environment*, 207, Part B, 108478.

Zhou, B., Rybski, D., Kropp, J. P. (2013). On the statistics of urban heat island intensity. *Geophys. Res. Lett.*, 40, 5486–5491.